

This is a repository copy of *A DiCre recombinase-based system for inducible expression in Leishmania major*.

White Rose Research Online URL for this paper:

<http://eprints.whiterose.ac.uk/119532/>

Version: Accepted Version

---

**Article:**

Santos, Renato E R S, Silva, Gabriel L A, Santos, Elaine V et al. (4 more authors) (2017) A DiCre recombinase-based system for inducible expression in *Leishmania major*. *MOLECULAR AND BIOCHEMICAL PARASITOLOGY*. pp. 45-48. ISSN 0166-6851

<https://doi.org/10.1016/j.molbiopara.2017.06.006>

---

**Reuse**

Items deposited in White Rose Research Online are protected by copyright, with all rights reserved unless indicated otherwise. They may be downloaded and/or printed for private study, or other acts as permitted by national copyright laws. The publisher or other rights holders may allow further reproduction and re-use of the full text version. This is indicated by the licence information on the White Rose Research Online record for the item.

**Takedown**

If you consider content in White Rose Research Online to be in breach of UK law, please notify us by emailing [eprints@whiterose.ac.uk](mailto:eprints@whiterose.ac.uk) including the URL of the record and the reason for the withdrawal request.

1   **A DiCre recombinase-based system for inducible expression in *Leishmania***  
2   ***major***

3  
4

5   Renato E. R. S. Santos<sup>1</sup>, Gabriel L. A. Silva<sup>1</sup>, Elaine V. Santos<sup>1</sup>, Samuel M. Duncan<sup>2</sup>,  
6   Jeremy C. Mottram<sup>2,3</sup>, Jeziel D. Damasceno<sup>1\*</sup> and Luiz R. O. Tosi<sup>1\*</sup>

7  
8

9   <sup>1</sup>Department of Cell and Molecular Biology; Ribeirão Preto Medical School,  
10   University of São Paulo; Ribeirão Preto, SP, Brazil.

11

12   <sup>2</sup> Wellcome Centre for Molecular Parasitology, Institute of Infection, Immunity and  
13   Inflammation, University of Glasgow, United Kingdom.

14

15   <sup>3</sup>Centre for Immunology and Infection, Department of Biology; University of York;  
16   York, UK.

17

18   \* To whom correspondence should be addressed. [jezielbqi@gmail.com](mailto:jezielbqi@gmail.com) and  
19   [luiztosi@fmrp.usp.br](mailto:luiztosi@fmrp.usp.br) Tel: + 55 16 36023117; Fax: +55 16 36020728.

20

21

22

23   **Keywords:** DiCre recombinase; *Leishmania*; inducible expression; DNA damage  
24   response; 9-1-1 complex; Rad9-Rad1-Hus1.

25

26

27   **Abstract**

28         Here we present the establishment of an inducible system based on the  
29         dimerizable Cre recombinase (DiCre) for controlled gene expression in the protozoan  
30         parasite *Leishmania*. Rapamycin-induced DiCre activation promoted efficient flipping  
31         and expression of gene products in a time and dose-dependent manner. The DiCre  
32         flipping activity induced the expression of target genes from both integrated and  
33         episomal contexts broadening the applicability of the system. We validated the  
34         system by inducing the expression of both full length and truncated forms of the  
35         checkpoint protein Rad9, which revealed that the highly divergent C-terminal domain  
36         of Rad9 is necessary for proper subcellular localization. Thus, by establishing the  
37         DiCre-based inducible system we have created and validated a robust new tool for  
38         assessing gene function in *Leishmania*.

39  
40       The genus *Leishmania* encompasses over 20 species, including those that  
41   are the causative agents of devastating human diseases worldwide collectively called  
42   leishmaniasis [1]. The *Leishmania* genome is organized in directional gene clusters  
43   that may include hundreds of genes from which transcription occurs in a polycistronic  
44   fashion. No canonical RNA Pol II promoters have been identified in this parasite and  
45   gene expression regulation seems to have been devolved to post-transcriptional  
46   processes [2]. The remarkable genome plasticity of *Leishmania*, which leads to  
47   frequent genome rearrangements, not only impacts gene expression control, but also  
48   hinders the genetic manipulation of the parasite [3,4]. Therefore, a dependable and  
49   robust genetic toolkit is necessary for effective post-genomic functional studies in this  
50   protozoan.

51       Over the past decades, a collection of genetic manipulation tools for  
52   *Leishmania* has been introduced. For instance, transient and stable transfection,  
53   gene replacement and disruption, expression vectors and functional  
54   complementation and rescue are well-established and reliable tools [5–7]. More  
55   recently, the introduction of protein stabilization strategies [8,9] a tetracycline-  
56   inducible system for protein expression [10], the dimerizable Cre recombinase  
57   (DiCre)-based system for inducible knockouts [11,12] and the establishment of  
58   CRISPR cas9 genome editing [13] has further improved our capacity to address  
59   peculiar aspects of this parasite's biology. Given the stringent regulation of DiCre  
60   recombinase activity and the variety of strategies for genetic regulation conferred by  
61   the use of loxP recombination sites [14,15], we decided to adapt the DiCre-based  
62   inducible system for controlled gene expression in *Leishmania major*. Our strategy  
63   involves the generation of a cell line constitutively expressing DiCre recombinase and  
64   carrying an inverted gene of interest flanked by *cis* orientated loxP sites. These  
65   constructs are integrated into the 18S rRNA locus and expressed under the control of  
66   the Pol I promoter. The antisense orientation of the gene of interest prevents  
67   transcription of coding RNA from the positive strand until activation of DiCre  
68   recombinase activity by rapamycin treatment. Once activated, DiCre catalyzes the  
69   'flip' of the sequence flanked by *cis* loxP sites, resulting in transcription of a coding  
70   RNA and subsequent protein expression (Figure S1A). To prevent continual gene  
71   'flipping' by loxP site recombination we employed left-element mutant (lox66) and  
72   right-element mutant (lox77) sites [16]. These mutated lox sequences act as sites of  
73   recombination to generate a wild-type loxP site and a double mutant Lox72 site for  
74   which DiCre has a dramatically reduced affinity. As such, a single recombination

75 event is favoured upon DiCre recombinase induction, thereby preventing re-  
76 inversion, leading to continual expression of the gene of interest (Figure S1B).

77 The advantages of this approach include: (i) the use of fewer transfection  
78 rounds and, consequently, fewer selectable markers when compared to the  
79 tetracycline-inducible system developed for *L. mexicana* by Kraeva and colleagues  
80 [10]; (ii) the possibility to induce expression of gene products from both chromosomal  
81 and/or episomal contexts; (iii) the system promotes a non-leaky expression that can  
82 be induced in a time and dosage-dependent manner; (iv) the possibility to compare  
83 the expression of endogenous and mutated proteins including the conditional  
84 expression of deleterious gene products.

85 To create the system, plasmid pGL2339 (Figure S2A) was digested and the  
86 array encoding the blasticidin resistance cassette and the dimerizable Cre  
87 recombinase subunits was integrated into the ribosomal locus to generate the  
88 DiCre<sup>SSU</sup> cell line (Figures 1A and Table S2). Next, the plasmid pGL2332 (Figure  
89 S2B) was digested and the lox66/lox77-flanked 6xHA-GFP cassette containing the  
90 puromycin resistance marker was integrated into the ribosomal locus of the DiCre<sup>SSU</sup>  
91 cell line to generate the GFP<sup>flox</sup> cell line (Figures 1B and Table S2). Both integration  
92 events were confirmed by PCR analysis, which also ascertained that the 6xHA-GFP  
93 coding sequence was present in the antisense orientation in the GFP<sup>flox</sup> cell line  
94 (Figure 1C). To test the system and the DiCre flipping activity, the GFP<sup>flox</sup> cell line  
95 was incubated with the DiCre dimerization ligand, rapamycin, and the inversion of the  
96 GFP cassette was confirmed by PCR analysis using the appropriate set of primers  
97 (Figure 1D). Semi-quantitative PCR analysis showed that the flipping reaction is time  
98 dependent and seem to reach its maximal level around 96 hours after induction  
99 (Figure S3). Importantly, flipping of the GFP cassette in the absence of rapamycin  
100 was not detectable in the PCR analyses shown in Figure 1D or Figure S3, indicating  
101 a non-leaky DiCre activity in the GFP<sup>flox</sup> cells. Upon rapamycin induction, expression  
102 of 6xHA-GFP was detectable after 12 hours and its levels were dose and time-  
103 dependent (Figure 1E). Consistently, 6xHA-GFP was not detectable in the absence  
104 of rapamycin, further confirming the stringent regulation of the system (Figure 1E).  
105 We further used immunofluorescence analysis (IFA) to examine the expression  
106 profile within the population and observed that 6xHA-GFP was detectable by IFA only  
107 after rapamycin incubation (Figure 1F). Consistent with the western blot analysis, the  
108 IFA also demonstrated the rapamycin dose-dependence of the system (Figure S3)  
109 further confirmed by the quantification of GFP corresponding signal (Figure 1G).  
110 Besides confirming the tight regulation of the system, this set of data also

111 demonstrates that the system is suitable for subcellular compartmentalization studies  
112 in this parasite.

113 To expand the limits of the system we tested it for the ability to flip sequences  
114 from an episome, which can be found in multiple copies in the cell. To that end, the  
115 plasmid pGL2332 was transfected into the DiCre<sup>SSU</sup> cell line to generate the pGFP<sup>flox</sup>  
116 cell line (Figure 1H). PCR analysis confirmed the DiCre background and the  
117 presence of the target plasmid (Figure 1I), and the flipping of the 6xHA-GFP cassette  
118 upon rapamycin incubation (Figure 1J). Consistently, western blot analysis confirmed  
119 the expression of the cassette exclusively in rapamycin treated cells (Figure 1K).  
120 These results further demonstrate the tight control of DiCre activity and greatly  
121 extend the applicability of the system as a reliable tool for inducible protein  
122 expression not only from the genomic context, but also from episomal targets. It is  
123 noteworthy that this system it is not expected to be reversible, which can be a  
124 disadvantage if reversion of the expressed phenotype is required. However, the  
125 irreversibility of the system can be taken an advantageous feature to be explored in  
126 both *in vitro* and *in vivo* infections assays where inclusion of selection drugs and  
127 rapamycin might not be desired.

128 To further validate the DiCre flipping tool we used the protein Rad9, which  
129 participates in the *Leishmania* DNA Damage Response as part of the checkpoint  
130 clamp 9-1-1 [17,18]. In eukaryotic cells, Rad9 has an unstructured C-terminal domain  
131 that corresponds to ~1/3 of the protein and is necessary for its function in signalling  
132 genotoxic stress [19]. The unstructured C-domain of *Leishmania* Rad9 is ~3.5x  
133 longer than its human counterpart (Figure 2A) and, so far, no function has been  
134 reported for this C-terminal extension. To start exploring the function of this C-  
135 terminal domain, Rad9 full length or C-terminal truncated encoding sequences, were  
136 cloned into the pGL6000 vector (Figure S2C), to generate the Rad9-6xHA<sup>flox</sup> and  
137 Rad9ΔC'-6xHA<sup>flox</sup> cassettes, respectively. These constructs were digested and  
138 integrated into the ribosomal locus of the DiCre<sup>SSU</sup> cell line to generate the Rad9<sup>flox</sup>  
139 and Rad9ΔC'<sup>flox</sup> cell lines, respectively (Figure 2B and Table S2). Proper Integration  
140 was confirmed by PCR analysis (Figure 2C) and, as expected, flipping of the  
141 cassettes was detected exclusively upon rapamycin incubation (Figure 2D).  
142 Accordingly, expression of Rad9-6xHA and Rad9ΔC'-6xHA was detectable at  
143 comparable levels after induction with rapamycin, as demonstrated by western blot  
144 analysis (Figure 2E; upper panel). Anti-Rad9 polyclonal serum was used in western  
145 blot analysis to evaluate changes in total Rad9 levels (i.e. Rad9-6xHA plus  
146 endogenous Rad9) in the Rad9<sup>flox</sup> cell line after DiCre activation (Figure 2E; middle

147 panel). Our analysis indicated that, upon induction, Rad9-6xHA was overexpressed  
148 when compared to the endogenous Rad9. Quantification of Rad9 signal revealed that  
149 up to ~65% of the total Rad9 expressed in these cells corresponded to the induced  
150 version of the protein demonstrating that the system can mediate overexpression.  
151 Interestingly, the induction of Rad9-6xHA resulted in significant decrease in the levels  
152 of endogenous Rad9. However, the same effect was less pronounced when the  
153 truncated Rad9 $\Delta$ C'-6xHA was expressed (Figure 2E; middle panel and Figure 2F).  
154 These data suggest that *Leishmania* Rad9 levels are under tight regulation, which  
155 probably involves the participation of its C-terminal extension. Whether this requires  
156 a direct or indirect role of this domain remains to be investigated. We were not able  
157 to properly assess Rad9 $\Delta$ C'-6xHA levels relative to endogenous Rad9 using the  
158 polyclonal anti-Rad9 serum. One reason for this is that anti-Rad9 serum detects a  
159 faster migrating protein with the same molecular mass as Rad9 $\Delta$ C'-6xHA, hindering  
160 its detection. Similarly to the endogenous Rad9, the level of this protein was also  
161 reduced upon induction of Rad9-6xHA (Figure 2E; middle panel). While the presence  
162 of this band could represent cross-detection of an unrelated protein, these data  
163 suggest that it could be a processed form of Rad9 and further characterization is  
164 needed to clarify this.

165 We also analysed the effect of the deletion of the C-terminal extension on the  
166 Rad9 subcellular localization. Using IFA, we observed that in the majority of the cells  
167 Rad9-6xHA was almost exclusively found in the nuclear compartment, as previously  
168 described for Rad9 [17] (Figures 2G and S4). On the other hand, truncated Rad9 $\Delta$ C'-  
169 6xHA presented a less defined localization being prominently detected in the  
170 cytoplasm of the majority of the cells (Figure 2G and S4). Consistently, quantitative  
171 analysis of the IFA data showed that Rad9-6xHA signal is concentrated in the region  
172 containing the nuclear DNA staining, while Rad9 $\Delta$ C'-6xHA signal expands beyond  
173 the nuclear staining limits (Figure 2H). Based on these data, it is reasonable to  
174 conclude that the C-terminal extension is necessary for proper subcellular distribution  
175 of Rad9 in *Leishmania*.

176 In summary, we have demonstrated that the DiCre-based expression system  
177 described here is a valuable addition to the *Leishmania* genetic manipulation toolkit.  
178 Its use to study the parasite Rad9 revealed important features of the protein,  
179 produced reagents for future studies and proved its value for functional analyses in  
180 this parasite.

181  
182 **Acknowledgments**

183 This work was supported by FAPESP - Fundação de Amparo à Pesquisa no  
184 Estado de São Paulo grants 14/06824-8, 14/00751-9, 13/00570-1 and 13/26806-1,  
185 the Medical Research Council (MR/K019384) and the Wellcome Trust [104111]. The  
186 Confocal Microscopy Laboratory was supported by FAPESP 04/08868-0. The  
187 Multiphoton Microscopy Laboratory was supported by FAPESP 09/54014-7. Roberta  
188 Ribeiro Costa Rosales and Elizabete Rosa Milani for assistance with microscopy  
189 experiments.

190

## 191 **Author contribution**

192 RERSS performed the experiments, collected data, and critically revised the  
193 manuscript. GLAS generated and analysed the pGFP<sup>flox</sup> cell line. EVS conducted the  
194 anti-Rad9 western blot analysis in Figure 2E. SMD and JCM generated pGL2332 and  
195 pGL2339 plasmids, provided reagents and critically revised the manuscript. JDD  
196 generated the DiCre<sup>SSU</sup> cell line, planned experiments, performed analysis presented  
197 in Figure 2A, helped acquire data of Figure 2G and wrote the manuscript. LROT  
198 planned experiments and wrote the manuscript.

199

200

## 201 **References**

202

- 203 [1] J. Alvar, I.D. Vélez, C. Bern, M. Herrero, P. Desjeux, J. Cano, J. Jannin, M.  
204 den Boer, the W.L.C. Team, Leishmaniasis Worldwide and Global Estimates  
205 of Its Incidence, *PLoS One.* 7 (2012) e35671.  
206 doi:10.1371/journal.pone.0035671.
- 207 [2] S. Martínez-Calvillo, S. Yan, D. Nguyen, M. Fox, K. Stuart, P.J. Myler,  
208 Transcription of *Leishmania major* Friedlin Chromosome 1 Initiates in Both  
209 Directions within a Single Region, *Mol. Cell.* 11 (2003) 1291–1299.
- 210 [3] J.-M. Ubeda, D. Légaré, F. Raymond, A. Ouameur, S. Boisvert, P. Rigault, J.  
211 Corbeil, M.J. Tremblay, M. Olivier, B. Papadopoulou, M. Ouellette, Modulation  
212 of gene expression in drug resistant *Leishmania* is associated with gene  
213 amplification, gene deletion and chromosome aneuploidy, *Genome Biol.* 9  
214 (2008) R115.
- 215 [4] M.B. Rogers, J.D. Hilly, N.J. Dickens, J. Wilkes, P.A. Bates, D.P. Depledge,  
216 D. Harris, Y. Her, P. Herzyk, H. Imamura, T.D. Otto, M. Sanders, K. Seeger,  
217 J.-C. Dujardin, M. Berriman, D.F. Smith, C. Hertz-Fowler, J.C. Mottram,  
218 Chromosome and gene copy number variation allow major structural change  
219 between species and strains of *Leishmania.*, *Genome Res.* 21 (2011) 2129–  
220 42.
- 221 [5] J.H. LeBowitz, C.M. Coburn, S.M. Beverley, Simultaneous transient  
222 expression assays of the trypanosomatid parasite *Leishmania* using β-  
223 galactosidase and β-glucuronidase as reporter enzymes, 1991.
- 224 [6] J.D. Damasceno, S.M. Beverley, L.R.O. Tosi, A transposon toolkit for gene  
225 transfer and mutagenesis in protozoan parasites., *Genetica.* 138 (2010) 301–  
226 11.
- 227 [7] J.N.G.. M.J.. Duncan S.M, Recent advances in reverse genetics of  
228 *Leishmania*: manipulating a manipulative parasite., Unpubl. Data. (2017).

- 229 [8] L. Madeira da Silva, K.L. Owens, S.M.F. Murta, S.M. Beverley, Regulated  
230 expression of the *Leishmania major* surface virulence factor  
231 lipophosphoglycan using conditionally destabilized fusion proteins, Proc. Natl.  
232 Acad. Sci. U. S. A. 106 (2009) 7583–8.
- 233 [9] L. Podešová, H. Huang, V. Yurchenko, Inducible protein stabilization system  
234 in *Leishmania mexicana*, 2017.
- 235 [10] N. Kraeva, A. Ishemgulova, J. Lukeš, V. Yurchenko, Tetracycline-inducible  
236 gene expression system in *Leishmania mexicana*, 2014.
- 237 [11] S.M. Duncan, E. Myburgh, C. Philipon, E. Brown, M. Meissner, J. Brewer, J.C.  
238 Mottram, Conditional gene deletion with DiCre demonstrates an essential role  
239 for CRK3 in *Leishmania mexicana* cell cycle regulation, Mol. Microbiol. 100  
240 (2016) 931–944.
- 241 [12] T. Beneke, R. Madden, L. Makin, J. Valli, J. Sunter, E. Gluenz, A CRISPR  
242 Cas9 high-throughput genome editing toolkit for kinetoplastids, R. Soc. Open  
243 Sci. 4 (2017).
- 244 [13] F.A. Ran, P.D. Hsu, J. Wright, V. Agarwala, D.A. Scott, F. Zhang, Genome  
245 engineering using the CRISPR-Cas9 system, Nat. Protoc. 8 (2013) 2281–  
246 2308.
- 247 [14] G.D. Van Duyne, A Structural View of Cre- *loxP* Site-Specific Recombination,  
248 Annu. Rev. Biophys. Biomol. Struct. 30 (2001) 87–104.
- 249 [15] N. Jullien, F. Sampieri, A. Enjalbert, J.-P. Herman, Regulation of Cre  
250 recombinase by ligand-induced complementation of inactive fragments.,  
251 Nucleic Acids Res. 31 (2003) e131.
- 252 [16] H. Albert, E.C. Dale, E. Lee, D.W. Ow, Site-specific integration of DNA into  
253 wild-type and mutant lox sites placed in the plant genome., Plant J. 7 (1995)  
254 649–59.
- 255 [17] J.D. Damasceno, V.S. Nunes, L.R.O. Tosi, LmHus1 is required for the DNA  
256 damage response in *Leishmania major* and forms a complex with an unusual  
257 Rad9 homologue, Mol. Microbiol. 90 (2013) 1074–1087.
- 258 [18] J.D. Damasceno, R. Obonaga, E. V. Santos, A. Scott, R. McCulloch, L.R.O.  
259 Tosi, Functional compartmentalization of Rad9 and Hus1 reveals diverse  
260 assembly of the 9-1-1 complex components during the DNA damage response  
261 in *Leishmania*, Mol. Microbiol. 101 (2016) 1054–1068.
- 262 [19] V.M. Navadgi-Patil, P.M. Burgers, The unstructured C-terminal tail of the 9-1-1  
263 clamp subunit Ddc1 activates Mec1/ATR via two distinct mechanisms., Mol.  
264 Cell. 36 (2009) 743–53.
- 265

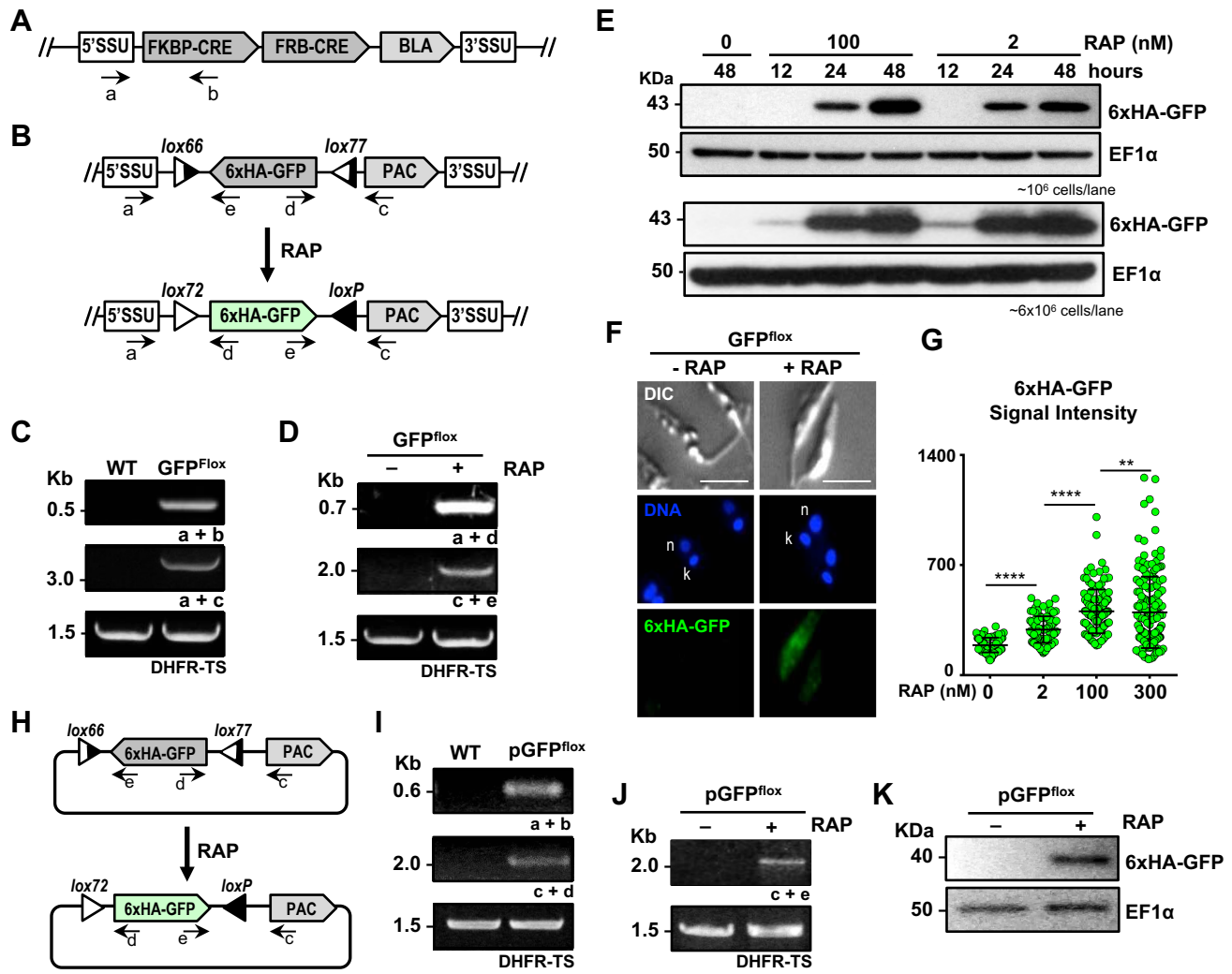
266 **Legends to Figures**

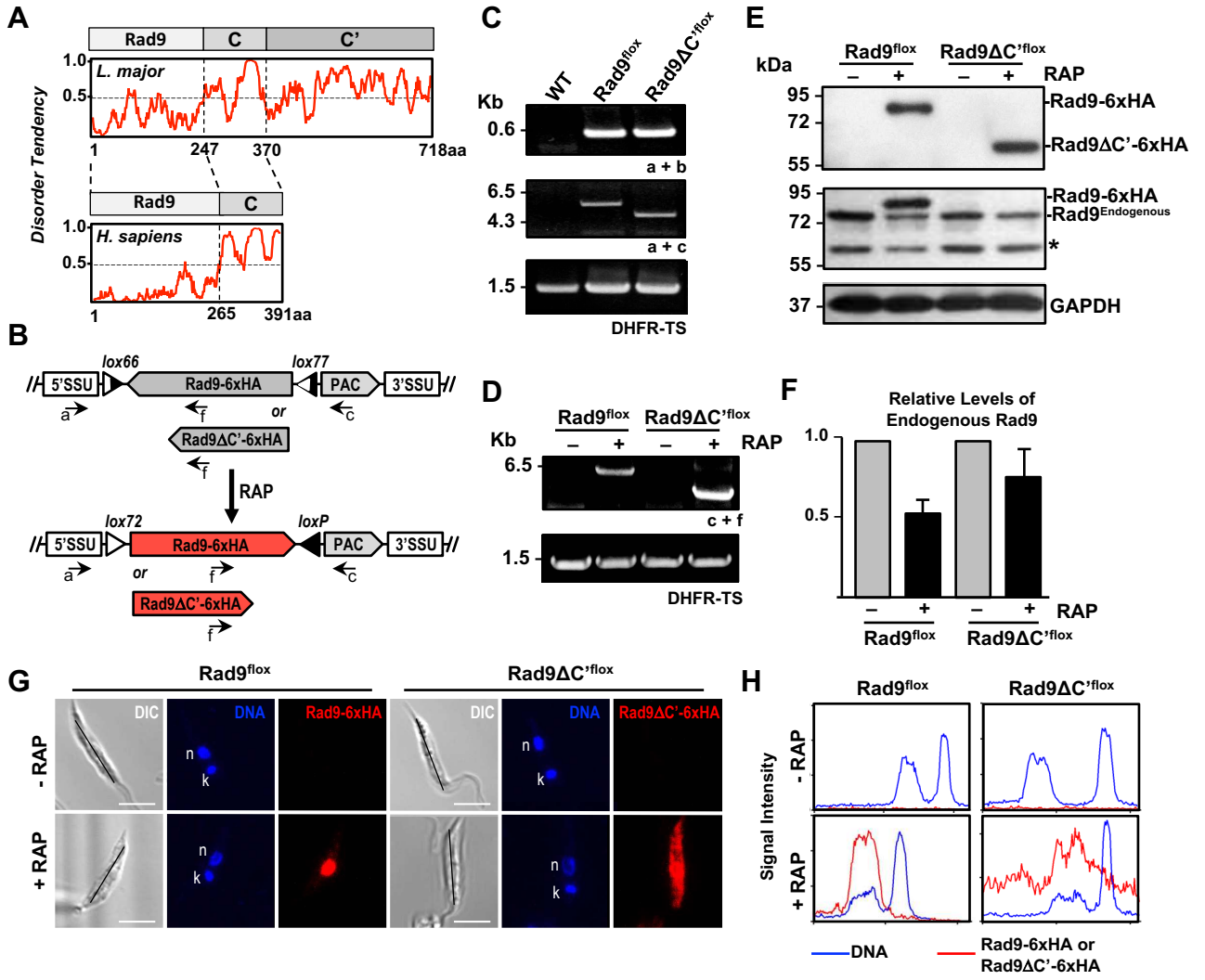
267

268 **Figure 1. Establishment of an inducible DiCre-based expression system in *L.***

269 **major. (A)** Schematic representation (not in scale) of the cassette encoding the  
270 truncated forms of DiCre after integration into the 18S ribosomal RNA locus (SSU) of  
271 *L. major* wild type cell (LT252) to generate the DiCre<sup>SSU</sup> cell line; BLA: blasticidin  
272 resistance marker. **(B)** Schematic representation (not in scale) of the 6xHA-GFP  
273 cassette (see Figure S1B for details) after integration into the SSU locus of the  
274 DiCre<sup>SSU</sup> cell line (A) to generate the GFP<sup>flox</sup> cell line; PAC: puromycin resistance  
275 marker; upon rapamycin (RAP) addition, the indicated lox sites mediate the flipping of  
276 6xHA-GFP cassette allowing its expression. In (A) and (B), black arrows indicate  
277 approximate annealing position of primers used for PCR analysis. **(C)** PCR analysis  
278 of genomic DNA (gDNA) using the indicated set of primers (annealing positions  
279 shown in (A) and (B)); DHFR-TS was the loading control for all PCR analyses  
280 presented in this work. **(D)** PCR analysis of gDNA from GFP<sup>flox</sup> cells cultivated in the  
281 presence (+) or absence (-) of 100nM RAP for 48h; primers are indicated below each  
282 panel (see annealing positions in (B)). **(E)** Western blot analysis of total cell extracts  
283 from the GFP<sup>flox</sup> cells cultivated with RAP for the indicated periods of time; two  
284 distinct cell-equivalent amount of extracts was analysed; anti-HA was used to detect  
285 6xHA-GFP; EF1 $\alpha$  was the loading control. **(F)** Immunofluorescence analysis of  
286 GFP<sup>flox</sup> cells cultivated in the presence (+) or absence (-) of 100nM RAP for 48h;  
287 images were acquired with a DMI 6000B inverted microscope (Leica); n and k  
288 indicate nuclear and kinetoplast DNA, respectively; scale bar = 5 $\mu$ m. **(G)** GFP<sup>flox</sup> cells  
289 were subject to immunofluorescence as in (F) after cultivation with RAP for 48h;  
290 signal corresponding to 6xHA-GFP from individual cells was quantified using Image J  
291 software; bars indicate mean +/- Standard Deviation (S.D.); p values by Kruskal-  
292 Wallis test were: (\*\*) = 0.0057; (\*\*\*) = 0.0008. **(H)** The plasmid pGL2332 (Figure  
293 S1B) was transfected as a circular episome in the DiCre<sup>SSU</sup> cells to generate the  
294 pGFP<sup>flox</sup> cell line; as in (B), RAP addition is expected to induce expression of 6xHA-  
295 GFP; schematic representations are not in scale. **(I)** PCR analysis of gDNA using the  
296 indicated set of primers (annealing positions shown in (A) and (H)). **(J)** PCR analysis  
297 of gDNA from pGFP<sup>flox</sup> cells cultivated in the presence (+) or absence (-) of 100nM  
298 RAP for 48h; primers are indicated below each panel (see annealing position in (H)).  
299 **(K)** Western blot analysis of total cell extracts from the pGFP<sup>flox</sup> cells cultivated in the  
300 presence (+) or absence (-) of 100nM RAP for 48h; anti-HA was used to detect  
301 6xHA-GFP; EF1 $\alpha$  was the loading control.

302  
303 **Figure 2. Expression of Rad9 and Rad9ΔC' using the DiCre-based inducible**  
304 **system.** **(A)** Predicted amino acid sequence of Rad9 from *L. major* (LmjF.15.0980)  
305 and *Homo sapiens* (NP\_004575.1) were subject to disorder prediction using IUPred  
306 (<http://iupred.enzim.hu>); values above 0.5 (horizontal black dotted line) can be  
307 considered as disordered regions; horizontal grey bars above each graph indicate  
308 the Rad9 domain (Pfam: PF04139) and the disordered C-terminal domain; C-terminal  
309 domain of human Rad9 and the corresponding region in *L. major* Rad9 is indicated  
310 as C; the extended C-terminal of *L. major* Rad9 is indicated as C'. **(B)** Full length  
311 Rad9 from *L. major* or a truncated version lacking the C-terminal extension (C'), were  
312 cloned as C-terminal fusion with a 6xHA tag to generated the Rad9-6xHA<sup>flox</sup> and  
313 Rad9ΔC'-6xHA<sup>flox</sup> constructs (not in scale); Rad9-6xHA and Rad9ΔC'-6xHA  
314 constructs are arranged in an inverted orientation, flanked by the indicated lox  
315 sequences and were integrated into the ribosomal locus (SSU) of the DiCre<sup>SSU</sup> cells  
316 (see Figure 1A) to generate the Rad9<sup>flox</sup> and Rad9ΔC'<sup>flox</sup> cell lines, respectively; black  
317 arrows indicate approximate annealing position of oligonucleotides used for PCR  
318 analyses; PAC: puromycin resistance marker. **(C)** PCR analysis of gDNA using the  
319 indicated set of primers (see annealing positions in (B)). **(D)** PCR analysis of gDNA  
320 from cells cultivated in the presence (+) or absence (-) of 100nM RAP for 48h;  
321 primers are indicated below each panel (see annealing positions in (B)). **(E)**  
322 Western blot analysis of total cell extracts from the indicated cells cultivated in the  
323 presence (+) or absence (-) of RAP for 48 hours; anti-HA (upper panel) and anti-  
324 Rad9 (bottom panel) was used to detect Rad9-6xHA Rad9ΔC'-6xHA; a protein with a  
325 similar migration pattern of Rad9ΔC'-6xHA is detected by anti-Rad9 and is indicated  
326 with (\*); GAPDH was the loading control. **(F)** Levels of endogenous Rad9 in western  
327 blot analysis shown in (E) were determined and normalized with the GAPDH signal,  
328 using Image J software; signal from cells exposed to RAP was plotted as a fraction  
329 relative to signal from respective non-induced culture. **(G)** Immunofluorescence  
330 analysis of the indicated cells cultivated in the presence (+) or absence (-) of 100nM  
331 RAP for 48h; images are representative of a Z-maximal projection from 14 Z-slices  
332 acquired with a multiphoton system coupled with LMS780 AxioObserver microscope  
333 (Zeiss); n and k indicate nuclear and kinetoplast DNA, respectively; black bars on the  
334 DIC field indicate the section where quantification shown in (H) was performed; n and  
335 k indicate nuclear and kinetoplast DNA, respectively; scale bar (white) = 5μm. **(H)**  
336 Signal corresponding to DAPI, Rad9-6xHA and Rad9ΔC'-6xHA in the section  
337 indicated by the black bar in (G) was quantified with ImageJ.





# Supplementary Information

## A DiCre recombinase-based system for inducible expression in *Leishmania*

Renato E. R. S. Santos<sup>1</sup>, Gabriel L. A. Silva<sup>1</sup>, Elaine V. Santos<sup>1</sup>, Samuel M. Duncan<sup>2</sup>, Jeremy C. Mottram<sup>2,3</sup>, Jeziel D. Damasceno<sup>1\*</sup> and Luiz R. O. Tosi<sup>1\*</sup>

<sup>1</sup>Department of Cell and Molecular Biology; Ribeirão Preto Medical School, University of São Paulo;  
Ribeirão Preto, SP, Brazil.

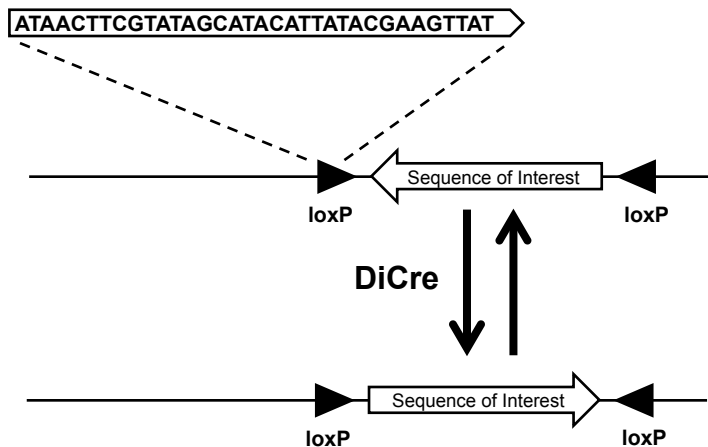
<sup>2</sup> Wellcome Centre for Molecular Parasitology, Institute of Infection, Immunity and Inflammation,  
University of Glasgow, United Kingdom.

<sup>3</sup>Centre for Immunology and Infection, Department of Biology; University of York; York, UK.

\* To whom correspondence should be addressed. [jezielbqi@gmail.com](mailto:jezielbqi@gmail.com) and  
[luiztosi@fmrp.usp.br](mailto:luiztosi@fmrp.usp.br) Tel: + 55 16 36023117; Fax: +55 16 36020728.

# Figure S1

**A**



**B**

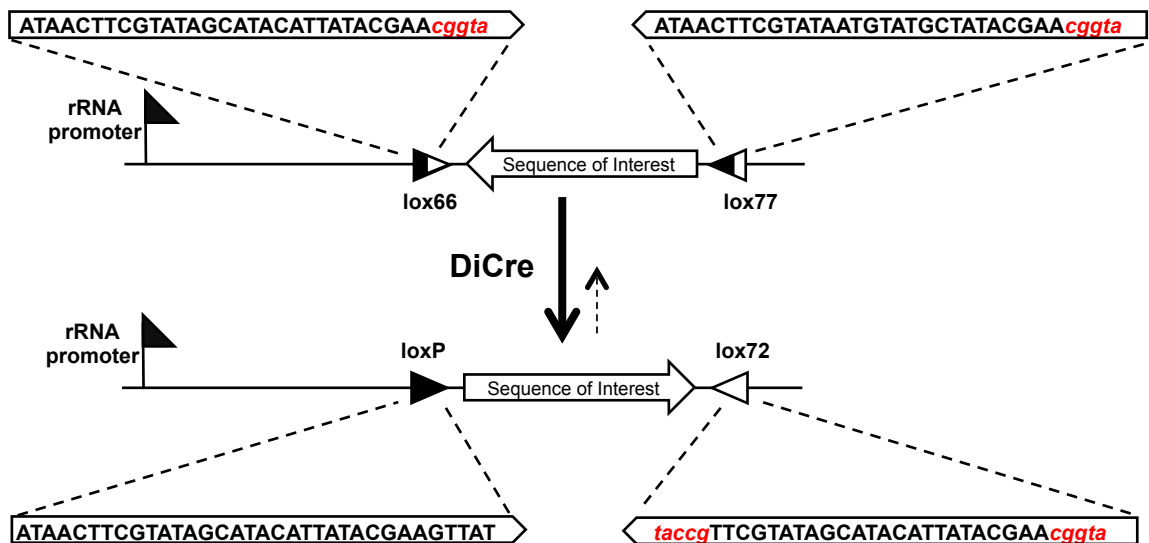


**Figure S1. Schematic description of the flipping activity catalysed by DiCre recombinase.**

**(A)** DiCre recognizes cis-inverted loxP sites and catalyse the inversion of any flanked sequence; the same loxP sequences are generated upon inversion, therefore re-inversion can proceed with the same efficiency; loxP sequence (5' to 3') is shown in the inset.

**(B)** Right and left mutated elements lox66 and lox77, respectively, are used to flank the sequence of interest; the sequences (5' to 3') for lox66 and lox77 are shown in the insets; red lower case indicate the mutated nucleotides; upon inversion, loxP and lox72 sequences are generated and re-inversion occurs at markedly reduced efficiency; upon inversion, P0II promoter-driven transcription of coding RNA from the positive strand mediates the expression of the gene of interest.

## Figure S2

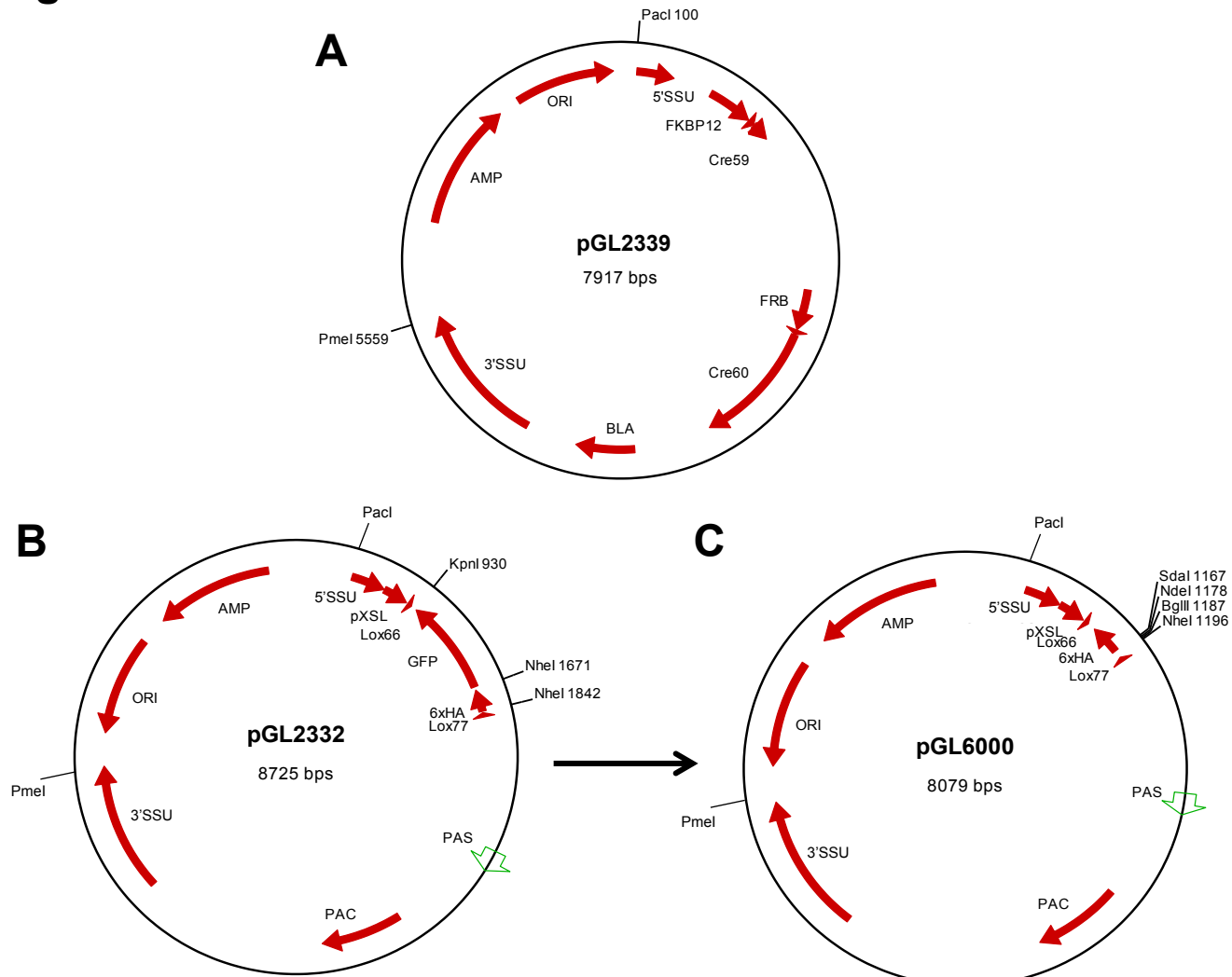


**Figure S2. Description of the plasmids and strategies used to generate the cell lines reported in this work.**

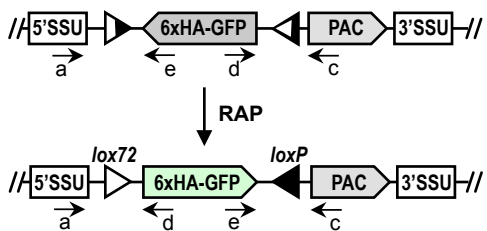
**(A)** pGL2339 plasmid bears the cassette encoding the inactive truncated forms of Cre-recombinase (DiCre) FKB12-Cre59 and FRB-Cre60; to generate the DiCre<sup>SSU</sup> cell line; the plasmid was digested with *PacI* and *Pmel* restriction enzymes and transfected into the *L. major* WT cell line (LT252); cells bearing the integration into the 18S ribosomal locus were cloned by serial dilution in M199 medium containing 10µg/ml blasticidin.

**(B)** pGL2332 plasmid bears the coding sequence for N-terminal 6xHA-tagged GFP; this fusion is inverted in relation to the 5' and 3' SSU sequences, and flanked by lox66 and lox77 sites; to generate the GFP<sup>flx</sup> cell line, pGL2332 was digested with *PacI* and *Pmel* restriction enzymes and transfected into the DiCre<sup>SSU</sup> cell line; cells bearing the integration into the 18S ribosomal locus were cloned by serial dilution in M199 medium containing 10µg/ml puromycin and 10µg/ml blasticidin.

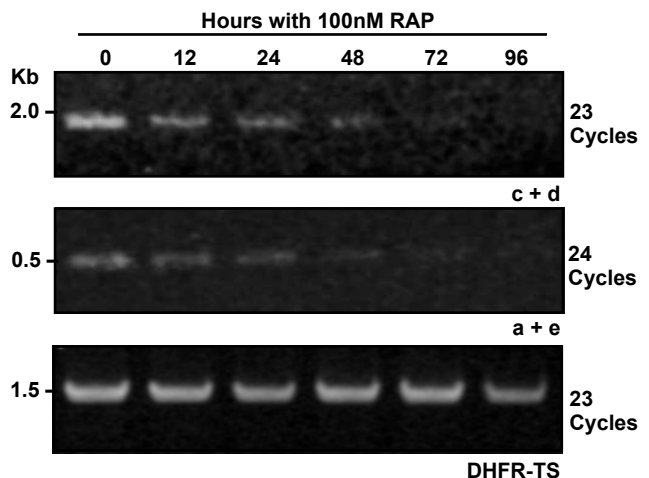
**(C)** To generate pGL6000 plasmid, pGL2332 was digested with *KpnI* and *NheI* restriction enzymes to remove the 6xHA-GFP coding sequence and ligated to a PCR product bearing the 6xHA tag and a multiple cloning site containing *Sdai*, *Ndel* and *BgII* restriction sites; the resulting vector allows for cloning of genes of interest as a C-terminal 6xHA fusion flanked by the lox66/lox77 sites; to generate the pGL6002 and pGL6004 plasmids, PCR products of the coding sequence for the full length or C-terminal truncated Rad9, respectively, were cloned into *Sdai* and *Ndel* restriction sites of the pGL6000 plasmid; to generate the Rad9<sup>flx</sup> and Rad9<sup>ΔC'flx</sup> cell lines, pGL6002 and pGL6004 plasmids, respectively, were digested with *PacI* and *Pmel* restriction enzymes and transfected into the DiCre<sup>SSU</sup> cell line; selection and cloning of transfectant parasites was done as in (B).

## Figure S3

**A**



**B**



**C**

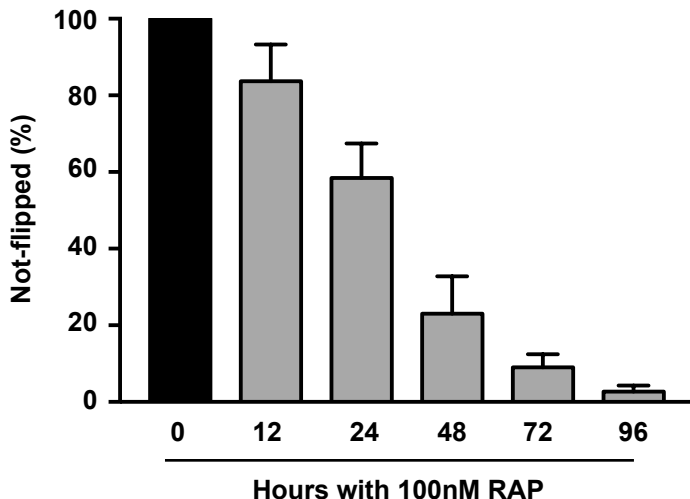


**Figure S3. Time course analysis of DiCre-mediated flipping efficiency.**

**(A)** Schematic representation (not in scale) of the 6xHA-GFP cassette after integration into the SSU locus of the DiCre<sup>SSU</sup> cell line to generate the GFP<sup>flx</sup> cell line; PAC: puromycin resistance marker; upon rapamycin (RAP) addition, the indicated lox sites mediate the flipping of 6xHA-GFP cassette allowing its expression; a, c, d and e indicate approximate annealing position of oligonucleotides used for the PCR analyses shown in (B).

**(B)** Genomic DNA (gDNA) was extracted from GFP<sup>flx</sup> cell line after cultivation with 100nM RAP for the indicated period time; ~ 10ng of gDNA was subjected to semi-quantitative PCR analysis using the indicated set of primers; ~15% of the PCR reaction was resolved in agarose gels; the number of cycles performed in each PCR reaction is indicated at right; annealing position for primers c+d and a+e, which detect only the molecules that has not been flipped, is shown in (A); DHFR-TS was used as the loading control.

**(C)** Signal corresponding to PCR products using primers c+d and a+e shown in (A) was measured using Image J software and then normalized with DHFR-TS signal; mean values obtained with each set of primers were calculated for each time point and are expressed relative to the 0 hours time point; vertical lines indicate standard error of the mean.

## Figure S4

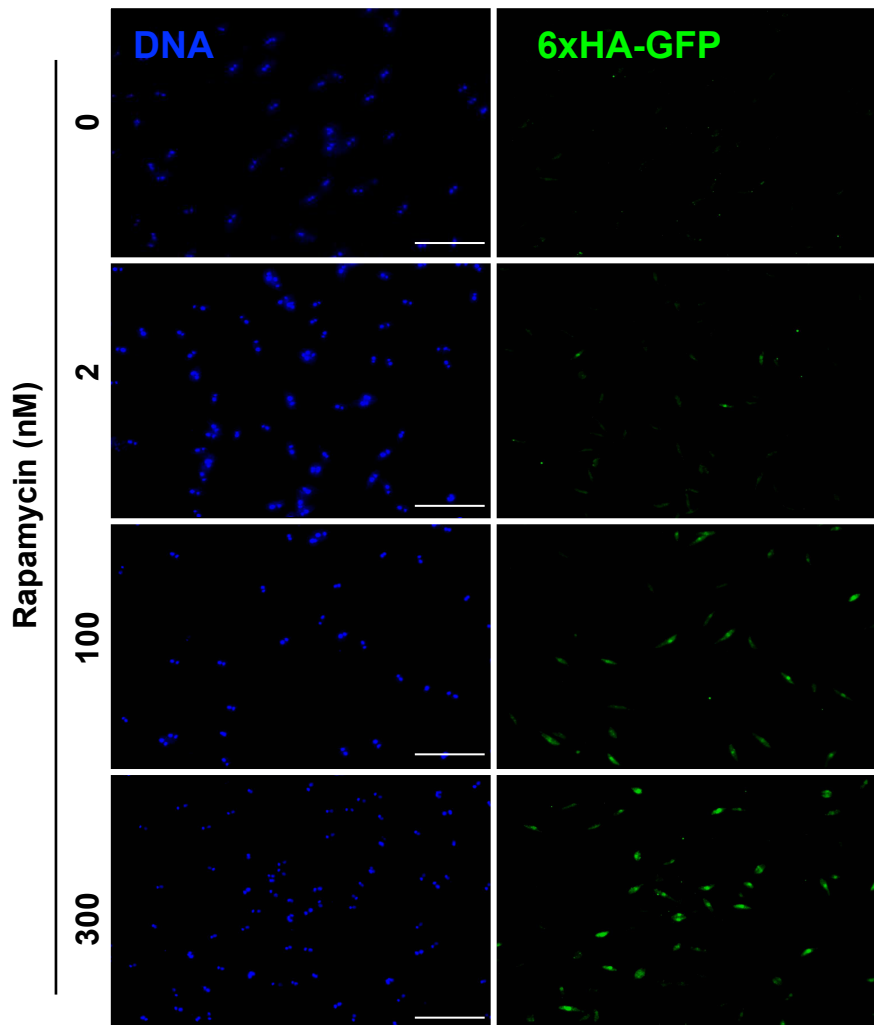


**Figure S4.** GFP<sup>flox</sup> cell line was cultivated in the presence of the indicated rapamycin concentrations for 48 hours; cells were fixed and subjected to immunofluorescence analysis using mouse anti-HA as primary antibody and anti-mouse conjugated with Alexa-Fluor 488 as secondary antibody (false coloured green); images were acquired with a DMI 6000B inverted microscope (Leica); scale bar = 25 $\mu$ m

## Figure S5

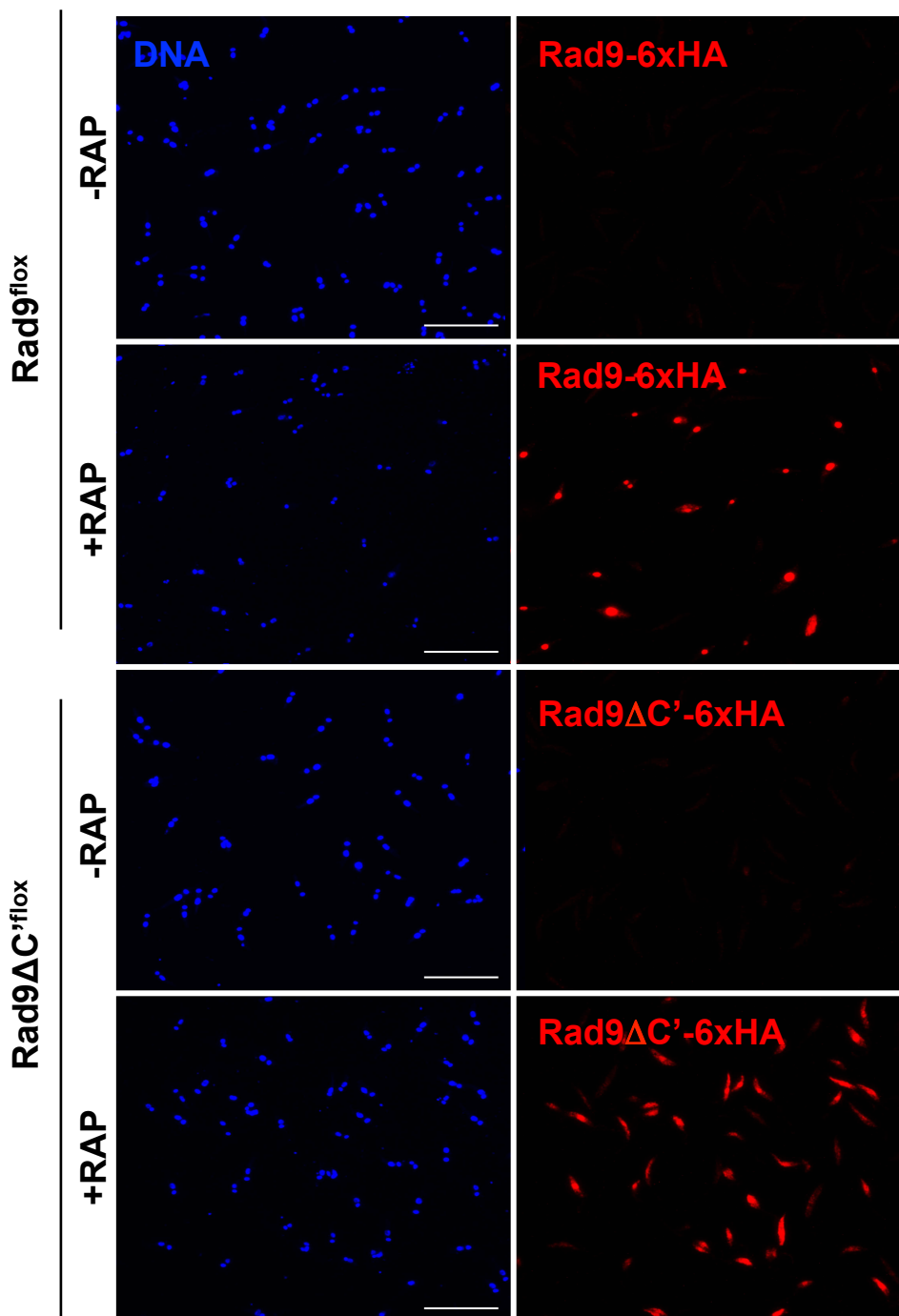


**Figure S5.** *Rad9<sup>flox</sup>* and *Rad9ΔC'<sup>flox</sup>* cell lines were cultivated in the presence (+) or absence (-) of rapamycin for 48 hours; cells were fixed and subjected to immunofluorescence analysis using mouse anti-HA as primary antibody and anti-mouse conjugated with Alexa-Fluor 488 as secondary antibody; images were acquired as a series of 14 Z-slices with a multiphoton system coupled with LMS780 AxioObserver microscope (Zeiss); images are representative of a Z-maximal projection from 14 Z-slices; scale bar = 25 $\mu$ m.

<b>Supplementary Table 1: Primers used in this work</b>		
<b>Designation in text</b>	<b>Sequence (5' → 3')</b>	<b>Reference</b>
a	CATTCGGTGCAGAAAGCCGG	Duncan <i>et al.</i> , 2016
b	GATGGTTCCACCTGCAC	
c	CCGTGGGCTTGACTCGGTCA	
d	CTGCCCTGTCACCAT	This work
e	GGCATGGACGAGCTGTACAAG	
f	ATTCTCGAGATGTCACTCCAATTACAGTGAG ( <i>Xba</i> I Site)	
Rad9NdelFw	ATTCATATGATGTCACTCCAATTACAGTGAG ( <i>Nde</i> I site)	
Rad9ABCsdalRv	ATT CCTGCAGGGTTCTGCCCTCGCGACAT ( <i>Sdal</i> site)	
Rad9ABSdalRv	ATT CCTGCAGGTGGCAGCGGAATGAAGCCGGCTG ( <i>Sdal</i> site)	
DHFR_Flank_Fw	ATGCCCGGGCATATGTCAGGGCAGCTCGAGGTTT	
DHFR_Flank_Rv	ATGCCCGGGCATATGCTATA CGGCCATCTCCATCTT	

<b>Supplementary Table 2: Cell lines used in this work</b>	
<b>Designation in text</b>	<b>Genetic nomenclature</b>
DiCre <sup>SSU</sup>	SSU DiCre BLA
GFP <sup>flx</sup>	SSU DiCre BLA SSU lox66((6xHA::GFP) <sub>AS</sub> )lox77 PAC
pGFP <sup>flx</sup>	SSU DiCre BLA [lox66((6xHA::GFP) <sub>AS</sub> )lox77 PAC]
Rad9 <sup>flx</sup>	SSU DiCre BLA SSU lox66((Rad9::6xHA) <sub>AS</sub> )lox77 PAC
Rad9ΔC <sup>flx</sup>	SSU DiCre BLA SSU lox66((Rad9ΔC::6xHA) <sub>AS</sub> )lox77 PAC

\*AS = Anti Sense

# Experimental procedures

## Parasites culture

*L. major* LT252 (MHOM/IR/1983/IR) and all other cell lines were cultured as promastigotes at 26°C in M199 medium plus 10% heat-inactivated fetal bovine serum. Generation of cell lines was done using the transfection protocol previously described (Kapler *et al.*, 1990).

## PCRs and cloning

Genomic DNA was extracted with DNeasy Blood & Tissue Kit (QIAGEN) according to manufacturer instructions. PCRs were performed using Taq DNA Polymerase (Thermo) for products up to 2kb or Phusion® High-Fidelity DNA Polymerase (NEB) for products with more than 2kb.

For generation of pGL6002 plasmid, the sequence coding for the 718 amino acids of full length Rad9 was amplified from gDNA using Rad9NdelFw and Rad9ABCSDalRv as primers (Table S1). For generation of pGL6004 plasmid, the sequence coding for the first 370 amino acids of Rad9 was amplified from gDNA using Rad9NdelFw and Rad9ABSdalRv as primers (Table S1).

## Antibodies and western blotting analyses

Rabbit anti-LmRad9 antibody was previously described (Damasceno *et al.*, 2013) and was used at 1:3 000 dilution. Rabbit anti-GAPDH antibody was kindly provided by Dr. Paul Michels and was used at the 1:15 000 dilution. The commercial antibodies used were as follows: mouse anti-HA (Sigma-Aldrich) at 1:1000 dilution, mouse anti-EF1 $\alpha$  (Merck Millipore) at 1:50 000 dilution. HRP-conjugated anti-mouse and anti-Rabbit antibodies (GE Life Sciences) were used at 1:10 000 and 1: 30 000 dilution, respectively.

Unless otherwise indicated, total cell extracts equivalent to  $\sim$ 10<sup>6</sup> cells were resolved by SDS-PAGE, transferred to PVDF membrane (GE Life Sciences) and analyzed with the indicated antibodies. Bands were detected with ECL Prime Western Blotting Detection Reagent (GE Life Sciences) and visualized with Hyperfilm ECL (GE Life Sciences).

## Immunofluorescence

Cells were fixed with 4% paraformaldehyde for 10 min at room temperature. Fixed cells were adhered to poly-L-lysine coated glass slides and permeabilized with 0.3% Triton X-100 for 30 min. Cells were pre-blocked with 2% BSA in 1x PBS for 1 hour. Anti-HA antibody was used at 1:1000 dilution to detect 6xHA-GFP, Rad9-6xHA and Rad9 $\Delta$ C-6xHA. Primary antibody was visualized with anti-mouse secondary antibody conjugated with Alexa Fluor 488 or Alexa Fluor 594 (Invitrogen). Slides were mounted with ProLong® Gold Antifade Reagent (Thermo) and 2 $\mu$ g/mL Hoechst 33342 (Thermo).

# **Plasmids**

>pGL2339

**pGL2339 Features**

ORI	7197 - 7870
5'SSU	108 - 361
FKBP12	624 - 935
Cre59	981 - 1106
FRB	2178 - 2454
Cre60	2490 - 3344
BLA	3864 - 4259
3'SSU	4603 - 5558
AMP	6192 – 705

>pGL2332

**pGL2332 Features**

5'SSU	409 - 662
pXSL	663 - 850
Lox66	860 - 893
GFP	1652 – 936 C
6xHA	1841 – 1677 C
Lox77	1884 – 1851 C
PAS	2876
PAC	3578 - 4174
3'SSU	5518 - 6477
ORI	7462 – 6723 C
AMP	8525 – 7665 C

>pGL6000

**pGL6000 Features**

5'SSU	409 - 662
pXSL	663 - 850
Lox66	860 - 893
6xHA	1152 – 946 C
Lox77	1238 – 1205 C
PAS	2230
PAC	2932 - 3528
3'SSU	4872 - 5831
ORI	6816 – 6077 C
AMP	7879 – 7019 C